Baroclinic Instability in the Presence of Barotropic Jets

PETROS IOANNOU*

N. Erythrea, Athens, Greece

RICHARD S. LINDZEN

Center for Meteorology and Physical Oceanography, Massachusetts Institute of Technology, Cambridge, MA 02139

(Manuscript received 28 January 1986, in final form 20 June 1986)

ABSTRACT

A formalism is developed for the calculation of baroclinic instability for barotropically stable jets. The formalism is applied to jet versions of both the Eady and Charney problems. It is found that jets act to confine instabilities meridionally, thus internally determining meridional wave scales. Once this internally determined meridional scale is taken into account, results correspond plausibly to classical results without a jet.

Consideration of the effect of such instabilities on the mean flow shows that they act to concentrate the jet barotropically while simultaneously reducing baroclinicity.

1. Introduction

The problem of baroclinic instability is central to dynamic meteorology. Early studies (Charney, 1947, Eady, 1949) considered what we shall refer to as homogeneous shears: that is, shears independent of the cross flow direction. More generally, the basic unperturbed state was taken to be a zonal flow, $\bar{U}(z)$, independent of the meridional distance, y. In such problems the meridional scale was usually taken as infinite, although it could also be arbitrarily specified or set by boundaries imposed at specific values of y.

For at least two obvious reasons, a less cavalier approach to meridional structure is called for: (i) observed cyclonic disturbances are meridionally confined to the neighborhood of jet streams—indeed the jet streams, bent and distorted by planetary-scale waves, appear to determine the paths followed by the storms (Niehaus, 1980, 1981; Fredericksen, 1978); (ii) The observed meridional scales are typically so small as to contribute significantly to the total horizontal wavenumber, which in turn plays a major role in determining growth rate and phase speed for baroclinic instabilities.

It is helpful to illustrate the latter effect immediately with reference to the Charney problem. In this problem one considers the stability of a flow consisting in a constant homogeneous shear

$$\bar{u} = u_0 + mz$$

and a constant static stability (or, more precisely, constant Brunt–Väisälä frequency),

$$N^2 = \frac{g}{T}\left(\frac{d\bar{T}}{dz} + \frac{g}{Cp}\right)$$

to perturbations of the form

$$\psi = \psi(z)e^{ik(x-ct)}e^{ily}.$$

The solution to this problem (Charney, 1947; Kuo, 1979; Miles, 1964; Lindzen and Rosenthal, 1981; and many others) yields growth rates, kc_i and phase speeds c_r as functions of α [the total horizontal wavenumber; $\alpha = (k^2 + l^2)^{1/2}$]. An example of such results for ($c_r - u_0$) and c_i is shown in Fig. 1. The results shown are dimensional; characteristic values have been chosen for m and N^2 (i.e., $m = 2.05 \times 10^{-3}$ s^{-1} and $N^2 = 1.6 \times 10^{-4}$ s^{-2}). Commonly one interprets data solely in terms of zonal wavenumber, k; relatedly, in Fig. 1, one associates α with k, setting $l = 0$. This, however, is unjustified. If meridional structure is determined by the equator–pole distance, then $l \sim 0.3$; while if the wave is confined by the mean jet, $l \sim 1.6$. Figure 2 shows growth rate, kc_i, and relative phase speed, $c_r - U_0$, as functions of k for both these choices of l as well as for $l = 0$.

We see that the choice of l has a profound effect. Indeed for the choice corresponding to "jet confinement," the "neutral point" separating Charney from Burger modes disappears and growth rates for small values of k appear large. This is essentially the situation described by Hoskins and Revell (1981).

The point of the above discussion is simply to emphasize the importance of meridional structure. The remainder of this paper is devoted to a study of how the meridional structure of the basic flow helps determine the meridional structure of the unstable waves.

* Currently serving as a Chief Petty Officer in the Greek Navy.

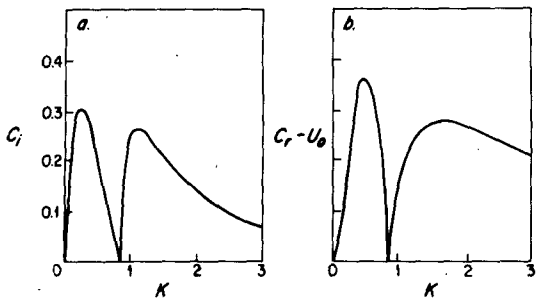

FIG. 1. (a) Nondimensional growth rate c_i and (b) relative phase speed $c_r - U$, where U is the zonal wind at the ground, as a function of nondimensional zonal wavenumber k. For reference, nondimensional $k = 1$ is equivalent to dimensional $k = 0.001$ km^{-1} and corresponds to dimensional wavelength 6400 km. Nondimensional phase speed $c = 1$ corresponds to dimensional $c = 60$ km h^{-1} and finally nondimensional time $t = 1$ to dimensional $t = 17$ h.

This question has already been addressed at length (Stone, 1969; Simmons, 1974; Gent, 1974; McIntyre, 1970; Killworth, 1980, 1981). These studies have, for the most part, been restricted to the Eady and 2-level type models. In the present paper we develop an analytically straightforward approach which, apart from a restriction to jets sufficiently broad (which is generally the case at middle and high latitudes), is general. The approach is applied to meridional jets in the contexts of both the Eady and the continuous Charney problems. The former allows comparison with earlier studies.

The development of our methodology is presented in section 2. The application to the Eady problem is given in section 3, and section 4 contains the application to the Charney problem.

We show that meridional jet structures do act to contain unstable eigenmodes meridionally. This containment can be sufficient to eliminate the existence of Burger modes. We also show that growth rates with basic meridional jets can be estimated from models without jets, provided one uses the vertical shear associated with the center of the jet and chooses an appropriate l. This choice, however, is not always clear. Relatedly, we find that there is a uniform transition to nonjet results as the jet is broadened.

Finally, in section 5 we calculate fluxes of heat and momentum associated with unstable waves. We find that these fluxes act to barotropically concentrate meridional jets while reducing mean baroclinicity.

2. Formulation and solution method

We will investigate the linear stability, with respect to quasi-geostrophic perturbations, of a zonal flow with velocity linear in height and "jet"-like in the meridional direction, $\bar{U} = z\bar{u}(y)$. The scale-height H and the Brunt–Väisälä frequency are constant. The effects of sphericity are confined to the beta-plane approximation. In what follows, the notation of Lindzen et al. (1980) will be used.

Conservation of pseudopotential vorticity requires for the streamfunction

$$(z\bar{u}(y)-c)\left[\frac{\partial^2\psi}{\partial z^2}-\frac{\epsilon\psi}{4H^2}+\frac{\partial^2\psi}{\partial y^2}-k^2\psi\right]+\frac{\partial\bar{q}(y,z)}{\partial y}\psi=0 \tag{2.1}$$

where

z height
y northward distance
x eastward distance
N Brunt–Väisälä frequency, assumed constant with height
$\bar{u}$ vertical shear of mean velocity profile
ψ perturbation streamfunction
k east–west wavenumber
c phase speed
f_0 Coriolis parameter at 45° latitude

$H = RT/g$, the scale height

$$\tilde{\psi} = \psi(z,y)\exp\left[\frac{z}{2H}+ik(x-ct)\right]$$

$$\epsilon = [f_0/N]^2$$

$$\bar{q}_y(y,z) = \beta + \frac{\bar{u}(y)}{H} - z\frac{d^2\bar{u}}{dy^2}$$

$\beta = df/dy$, (we will be working on a beta-plane.)

{Note $[z\bar{u}(y)]_{zz} = 0$}

The boundary condition requires that the vertical velocity vanish at the ground or at a lid, i.e., at

$$z = h_i,\ (h_i\bar{u}(y)-c)\left[\frac{\partial\psi}{\partial z}+\frac{\psi}{2H}\right]-\bar{u}(y)\psi=0,\ i=1,2;$$

if h_2 is infinity, then ψ should tend to 0. Also, as $|y| \to \infty$, ψ should approach 0.

For a given basic flow $z\bar{u}(y)$ and a given wavenumber, we have an eigenvalue problem for the determination of c and its corresponding north–south and vertical structure.

We will consider mean zonal profiles, $\bar{u}(y)$, that are symmetric with respect to 45° latitude (corresponding also to the origin of the y-axis) and jetlike. This choice is suggested by observations.

To nondimensionalize, we set (prime signifies a nondimensional quantity)

$$z = Hz'$$

$$(z\bar{u}, c) = \bar{m}H(z'\bar{u}', c')$$

$$x = ax'$$

$$y = \left[\frac{NH}{f}\right]y' = ay'$$

$$k^2 = k'^2\frac{\epsilon}{H^2}$$

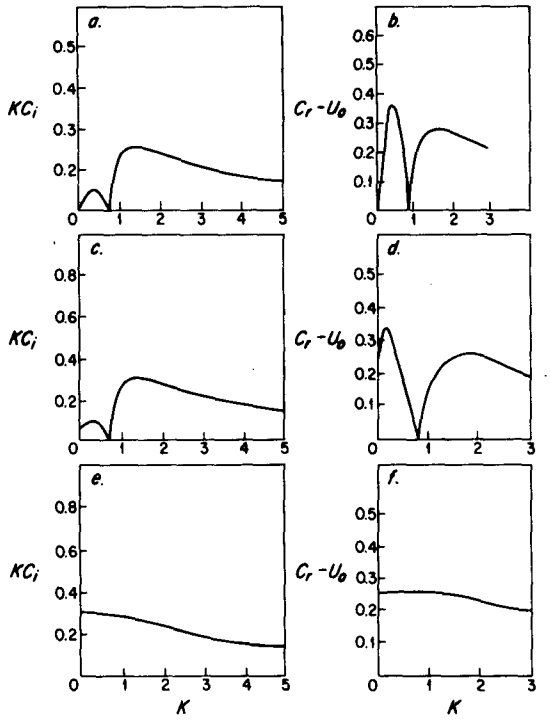

FIG. 2. Plot of growth rate, kc_i (a, c, e), and relative phase speed, $c_r - U$ where U is the zonal wind at the ground (b, d, f) as a function of zonal wavenumber, k; (a, b) are for the case of meridional wavenumber $l = 0$ (no meridional structure), (c, d) are for the case $l = 0.3$ (meridional structure with the scale of the pole to equator distance), and (e, f) are for the case of $l = 1.6$ (meridional structure with the scale of an observed midlatitude jet).

where a is Rossby radius of deformation and $\bar{m}$ the vertical shear at $y = 0$

On substitution, the nondimensional equations are (after dropping the primes)

$$(z\bar{u}(y)-c)\left[\frac{\partial^2\psi}{\partial z^2}+\frac{\partial^2\psi}{\partial y^2}-\mu^2\psi\right] + \left[r+\bar{u}(y)-z\frac{d^2\bar{u}(y)}{dy^2}\right]\psi=0. \quad (2.2)$$

At $z=\dfrac{h_i}{H}=h_i'$,

$$(h_i'\bar{u}(y)-c)\left[\frac{\partial\psi}{\partial z}+\frac{\psi}{2}\right]-\bar{u}(y)\psi=0, \quad i=1,2.$$

If $h_2/H \to \infty$ then $\psi \to 0$ and as $|y| \to \infty$, $\psi \to 0$ where $\mu^2 = k^2 + \frac{1}{4}$ and $r = \beta H/\epsilon\bar{m}$.

To this point, no unusual approximation has been introduced. In general, variation of the velocity profile with height and latitude leads to nonseparable equations, making the problem analytically intractable. To simplify matters, we will assume that the variation of the velocity profile with latitude is slow. Slow means that the velocity profile varies little in a distance of a Rossby radius of deformation. This is a realistic assumption for atmospheric and oceanic flows. Also, the treatments of this problem by Stone (1969), Gent (1974, 1975), Simmons (1974) and Killworth (1980) were developed under such an assumption. So if the scale of variation of $\bar{u}$ is denoted by L, we will consider the asymptotic limit of L tending to infinity.[1]

Defining the slow variable $Y = y/L$, we can apply a two-scaling formalism on the field equations as in Stone (1969), Gent (1974, 1975) and Killworth (1980, 1981),

$$\frac{\partial^2\psi}{\partial y^2}=\frac{\partial^2\psi}{\partial y^2}+\frac{2}{L}\frac{\partial^2\psi}{\partial y\partial Y}+\frac{1}{L^2}\frac{\partial^2\psi}{\partial Y^2} \quad (2.3)$$

and write the variable ψ as

$$\psi = W(y)\left[\psi_0(z,Y)+\frac{1}{L}\psi_1(z,Y) + \frac{1}{L^2}\psi_2(z,Y)+\cdots\right]. \quad (2.4)$$

This is a general expansion that leads to the quasi-separation of equation (2.2), and the accompanying corrections of c are

$$c = c_0+\frac{1}{L}c_1+\frac{1}{L^2}c_2+\cdots. \quad (2.5)$$

To zero order the equation assumes the form ($'$ denotes differentiation with respect to z):

$$\frac{\psi_0''}{\psi_0}-\mu^2+\frac{r+\bar{u}(Y)}{z\bar{u}(Y)-c}=-\frac{W_{yy}}{W}. \quad (2.6)$$

Given that the left-hand side of (2.6) is independent of y and the other side of the equation is independent of z, we must have (we again drop the subscripts)

$$\psi''+\left[\frac{r+\bar{u}(Y)}{z\bar{u}(Y)-c}-(\mu^2+l^2(Y))\right]\psi=0 \quad (A)$$

$$W_{yy}+l^2(Y)W=0 \quad (B)$$

Equivalently (B) can be written as

$$W_{YY}+L^2l^2(Y)W=0. \quad (B')$$

Our boundary conditions are

$$(h_i'\bar{u}(Y)-c)\left[\psi_z+\frac{\psi}{2}\right]-\bar{u}(Y)\psi=0$$

$$\text{at} \quad z=\frac{h_i}{H}=h_i', \quad i=1,2$$

[1] It is sometimes stated that this scaling filters out barotropic instability. This statement, while in some sense correct, is not totally meaningful in the present context. The existence of any instability requires that there exist a surface across which $\partial\bar{q}/\partial y$ (in Eq. 2.1) change sign (Charney and Stern, 1962). In pure baroclinic instability this surface is horizontal; in pure barotropic instability this surface is vertical. Our scaling demands that the surface be approximately horizontal.

If h_2/H is infinite $\psi \to 0$, then $|W| \to 0$ as $|\bar{Y}| \to \infty$. Note that (A) is the equation for the ordinary Charney problem; the Y dependence is only parametric.

It is informative to actually evaluate the parameters in our asymptotic analysis using typical numerical values. Evaluating f_0 and β at 45° latitude, we have, approximately,

$$f_0 = 10^{-4}\,\mathrm{s}^{-1}$$

$$\beta = 1.6\times 10^{-11}\,\mathrm{s}^{-1}\,\mathrm{m}^{-1}$$

$$\bar{m} = 2.05 * 10^{-3}\,\mathrm{s}^{-1}$$

$$N^2 = \frac{g}{T}\left(\frac{dT}{dz}+\frac{g}{C_p}\right) = 1.6\times 10^{-4}\,\mathrm{s}^{-2}$$

$$H = 8\times 10^3\,\mathrm{m}$$

$$a = 10^3\,\mathrm{km}$$

yielding $\epsilon = 0.625\times 10^{-4}$ and $r = 1.0$

Thus the nondimensional wavenumber (k or l) is related to the dimensional wavelength by

$$\text{wavelength} = \frac{6.28\times H}{\epsilon^{1/2}k} = \frac{6.4\times 10^3}{k}\ \text{km}.$$

We will be presenting our results in terms of the parameter Ros = $1/L$, which signifies how many times smaller the Rossby radius is than the half-width of the jet. The slow variable Y is related to the dimensional meridional distance y by

$$Y = \frac{y}{aL},$$

hence $Y = 1$ corresponds to $y = aL$.

The equator–pole distance is 10^4 km (as the metric system was defined to yield that), and from Fig. 3 the tropospheric jet has a typical half-width between (0.8–1.4) × 10^3 km, the pedestal (namely the value that the velocity profile asymptotes to at large distances from the center of the jet) is between 0.2–0.4, and the value of the wind at the center is typically 35 m s^{-1}. Hence Ros = 0.6–1.2. The assumption of small Ros seems marginal; however, the convergence of 2.4 and 2.5 will be checked a posteriori. Figure 3 also shows that the jet is, to a very good approximation, symmetric.

We have now reduced the nonseparable differential equation (2.1) to a set of weakly coupled one-dimensional equations; one in the vertical [Eq. (A)] and one in the latitudinal direction [Eq. (B)]. The vertical equation involves the two parameters c (complex phase speed) and $l^2(Y)$ (complex meridional wavenumber); in the traditional homogeneous case, l^2 is given, and we solve for c. In the present case (A) and its boundary conditions provide a functional relation between $l^2(Y)$ and c. However, only particular choices of c will lead to $l(Y)$ such that solutions to (B) will satisfy appropriate boundary conditions.

We can formulate a numerical iterative scheme for the determination of such a c. We start with a guess of c and determine $l(Y)$ by solving (A) and satisfying its boundary conditions. The $l(Y)$ now determines the coefficient of (B). We apply the shooting method to (B) marching from the north and south of the jet to a given latitude (if the jet is symmetric, this latitude can be taken to be the center of symmetry). The discrepancy in the slopes of the two marched solutions is the input to a Newton-iteration scheme that determines a new c. This scheme was found to rapidly converge, yielding a c and a corresponding streamfunction that decays exponentially far from the jet. It was further found that a good initial guess for c is the eigenvalue of the homogeneous baroclinic instability at the center of the jet with a meridional wavenumber characteristic of a disturbance confined in the neighborhood of the jet maximum. This process yields for each longitudinal wavenumber k the corresponding c and the variation of $l^2(Y)$.

This scheme was used to find the spectra of the nonuniform Charney problem. The numerical method in

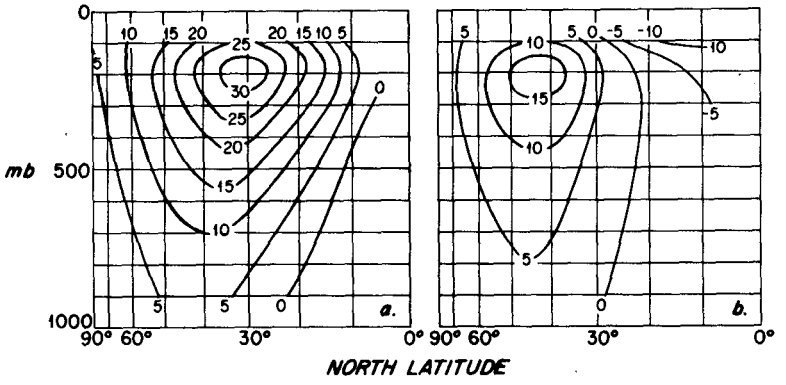

FIG. 3. A profile of the mean zonal wind (averaged in time and longitude) for (a) northern winter (December–February) and (b) northern summer (June–August). From Lorenz (1967, p. 35).

the case of the Charney problem is that of Lindzen and Kuo (1969). For simpler models of baroclinic instability (Eady and two-layer models) the solution process can be pursued nearly analytically. This is due to the fact that the functional relation between l^2 and c is easy enough so that direct integration of (B) may be possible, and approximate W.K.B.J. methods directly applicable (Gent 1974, 1975, Killworth, 1980). The W.K.B.J. approximation that we will describe in detail is useful as it clearly shows what is happening in the more complicated models like that of Charney.

In the case of a slowly varying jet, (B) is in the canonical form for a W.K.B.J. analysis (see Erdelyi, 1956). The condition that at large distances from the center of the jet the meridional shear vanishes, forces $l^2(Y, c)$ to be a constant there. With c and l^2 complex the solution as $|Y| \to \infty$, $W \sim \exp(\pm iLl(Y, c)Y)$, will be either exponentially increasing or decreasing. The boundary conditions then lead us to choose

$$W \to \exp(iLl(Y,c)Y) \quad \text{as} \quad Y \to \infty$$
$$W \to \exp(-iLl(Y,c)Y) \quad \text{as} \quad Y \to -\infty,$$

where $\mathrm{Im}(l(Y, c)) > 0$. The W.K.B.J. technique joins these two solutions and thus determines the eigenvalue c.

The asymptotic solution $W = \exp(iLl(Y, c)Y)$ is invalid near points Y_0 at which $l(Y_0, c) = 0$. These are the turning points. In our case, since l is a complex function, the turning points will be complex as well. Near Y_0, l can be expanded:

$$l(Y,c) = (Y - Y_0)\left[\frac{dl}{dY}\right]_{Y=Y_0} \tag{2.7}$$

and the solution to (B) near Y_0 will be:

$$W(Y) = p(Y-Y_0)^{1/2}J_{(1/3)}\left[\frac{2}{3}(Y-Y_0)^{3/2}L\frac{dl}{dY_0}\right] + q(Y-Y_0)^{1/2}J_{(1/3)}\left[\frac{2}{3}(Y-Y_0)^{3/2}L\frac{dl}{dY_0}\right]. \tag{2.8}$$

Here p, q are complex numerical factors to be determined from the boundary conditions.
From (2.7) we have

$$\int_{Y_0}^{Y} l\,dY = \frac{2}{3}(Y-Y_0)^{3/2}l' \tag{2.9}$$

for Y near Y_0 and $l' = (dl/dY)_{Y=Y_0}$; we see that these solutions join smoothly onto the asymptotic solution $\exp(iL \int l dY)$. It is also evident from the asymptotic expansions at $J_{(\pm 1/3)}(\int LldY)$ (the argument of the Bessel functions has been substituted by virtue of 2.9), that whatever linear combination is exponentially decreasing as $Y \to -\infty$ will diverge as $Y \to \infty$. Thus, we see that a bounded solution to (B) requires that complex $l(Y, c)$ have at least two zeros.

For a jet with a single maximum we in fact have two turning points, and it is only this case that we will present.

As is clear from (2.9), in the complex plane three rays S emanate from the turning point Y_0, and on these the solution is purely oscillatory; there also emanate three rays A on which the solution is exponential. The S rays are defined as the Y that obey

$$\mathrm{Im}\left(\int_{Y_0}^{Y} l(Y,c)dy\right) = 0. \tag{2.10}$$

The A rays are defined as the Y that obey

$$\mathrm{Re}\left(\int_{Y_0}^{Y} l(Y,c)dY\right) = 0. \tag{2.11}$$

Refer to Fig. 4a for details. We note that if one seeks the solution $W(Y)$ that decays as $|Y| \to \infty$, Y must lie in regions D_1 and D_2; if one specifically wants the solution to decay on the real axis of the complex Y plane, then the real axis must lie in the domain of D_1 and D_2 (as shown in Fig. 4a). Instead of solving Eq. (B) on the real axis, we solve it along the curve C consisting of

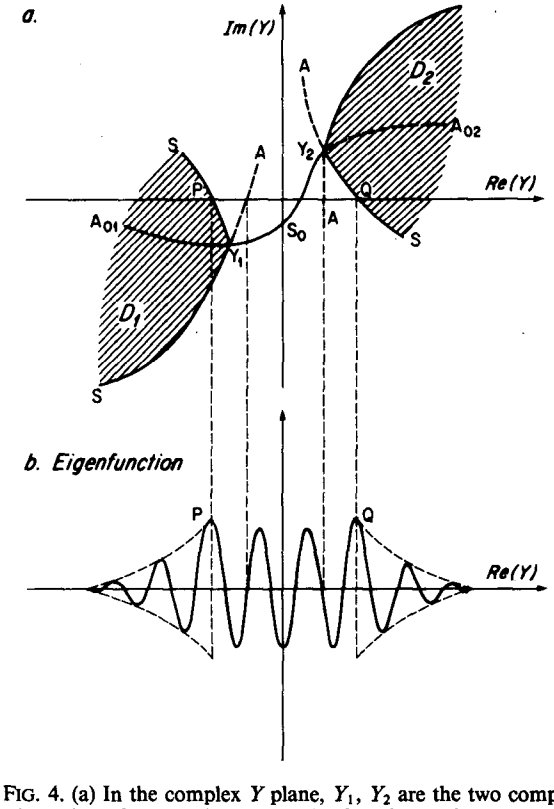

FIG. 4. (a) In the complex Y plane, Y_1, Y_2 are the two complex turning points of Eq. (B). We denote with S the Stokes lines emanating from them and with A the anti-Stokes lines. The two shaded regions D_1, D_2 are where the differential equation admits exponentially decaying solutions. (b) The real part of the eigenfunction, corresponding to the turning point configuration in (a), is plotted against the real latitude Y.

$A_{01} + S_0 + A_{02}$. On that curve $W(Y, c)$ is effectively real, and we can derive the eigencondition as in quantum mechanics (Bender and Orszag, 1978). We get;

$$L\int_{Y_1}^{Y_2} l(y,c)dY = \left(n+\frac{1}{2}\right)\pi, \quad n=0,\pm1,\pm2,\pm3,\cdots. \tag{2.12}$$

This is the eigenvalue relation for the baroclinic instability of the jet. In the case of no meridional shear, the dispersion relation is $l(c) = 0$. In distinction to quantum mechanics this integration takes place in the complex Y plane. The behavior of a typical eigensolution is shown in Fig. 4b.

The case of a symmetric jet offers some further simplifications. The meridional equation and boundary conditions are invariant under the transformation $Y \to -Y$. Thus the eigenfunctions will be either symmetric or antisymmetric.

Finally, there are two integral properties which can be derived. Multiplying (B) by W^* and integrating over Y we get

$$\int_{-\infty}^{\infty} |W_Y|^2 dY + \mathrm{Re}\left(\int_{-\infty}^{\infty} L^2 l^2(Y,c)|W|^2 dY\right) = 0 \tag{2.13}$$

$$\mathrm{Im}\left(\int_{-\infty}^{\infty} L^2 l^2(Y,c)|W|^2 dY\right) = 0. \tag{2.14}$$

In the case of symmetric jets, the above expressions are valid in the half domains $[0, \infty]$ and $[-\infty, 0]$. Conditions (2.13) and (2.14) are necessary conditions for the existence of a bounded solution to (B). Expressions (2.13) and (2.14) were used to test the numerical solutions that will be presented.

An interpretation of (2.14) will be described in section 5 where the effect of the eddies on the mean flow is discussed. As we shall see, (2.14) expresses conservation of momentum (i.e., the net exchange of momentum between the perturbation and the mean flow vanishes).

3. The Eady problem

We will demonstrate the use of the W.K.B.J. technique in the solution of the Eady problem. This problem was solved by Gent (1974, 1975). We will concentrate on the relation between the spectra of the homogeneous (Eady without meridional shear) and inhomogeneous (Eady with meridional shear) cases, a topic that is partially clarified by the previous investigators (refer also to McIntyre, 1970).

Apply the Boussinesq approximation to (A) (take $H = \infty$ and drop the term $r + 1$), place the ground at $-h/2$ and an upper lid at $h/2$. Consider a symmetric jet of the form $\bar{u}(Y) = 1/(1 + qY^2)$, $q > 0$.

At each meridional section, we have an Eady type instability problem. The stability problems at each section are connected through (B). The solution of (A) at each section yields the local dispersion relation (refer to Pedlosky, 1979, p. 458):

$$c^2 = \frac{\bar{u}^2(Y)}{d^2}\left[\frac{d}{2} - \coth\left(\frac{d}{2}\right)\right]\left[\frac{d}{2} - \tanh\left(\frac{d}{2}\right)\right]. \tag{3.1}$$

Here $d^2(Y) = k^2 + l^2(Y)$ (the ¼ is missing due to the Boussinesq approximation). For all real d, $d/2 > \tanh(d/2)$ and $c^2 < 0$ for $d < d_c = 2.3994$; the eigenvalue in other words is purely imaginary. For $d > d_c$ the eigenvalues are real and the solution describes two neutral waves. In Fig. 5 the dispersion for real d is plotted. Dispersion relation (3.1) has simple poles in the complex plane at $d = in\pi$, $n = \pm1, \pm2, \pm3, \cdots$ the negative integers are excluded, due to the choice of branch. Equation (B) takes the form:

$$W'' + L^2[d^2(Y) - k^2]W = 0. \tag{3.2}$$

Hence, by taking $d_c > d(0) > k$ and tracing the path G shown in Fig. 6, we can always obtain a purely imaginary c that makes W decay at infinity. The Eady problem has the fortunate property that the path (shown in Fig. 6) traced by $d(Y)$, as $u(Y)$ varies, is the same for all k. This does not happen in the Charney problem. Thus, all that matters in the Eady problem is the behavior of the dispersion in the region between k and $d(0)$. The situation is akin to the particle in the box in quantum mechanics, where for low energies, the behavior of the potential in the classically inaccessible regions is immaterial.

Thus, instead of dispersion relation (3.1), we consider

$$4c^2 \approx \bar{u}^2(Y)\left(1 - \frac{\pi^2 + d_c^2}{\pi^2 + d^2}\right). \tag{3.3}$$

Equation (3.3) is very close to (3.1). The eigenvalue relation for a symmetric jet, according to the previous section, is of the form:

$$2L\int_0^{Y_0} l(Y)dY = \left[n+\frac{1}{2}\right]\pi. \tag{3.4}$$

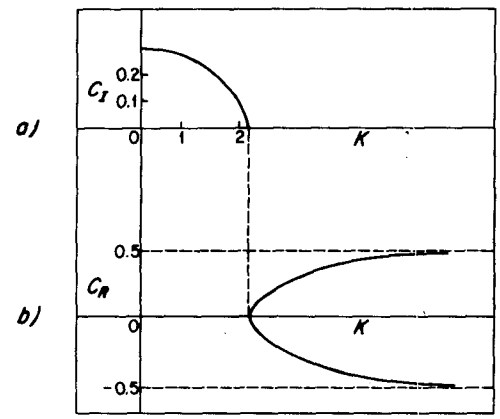

FIG. 5. For the homogeneous Eady problem: (a) growth rate c_i as a function of zonal wavenumber k; (b) phase speed c_r as a function of k. The variables are nondimensional.

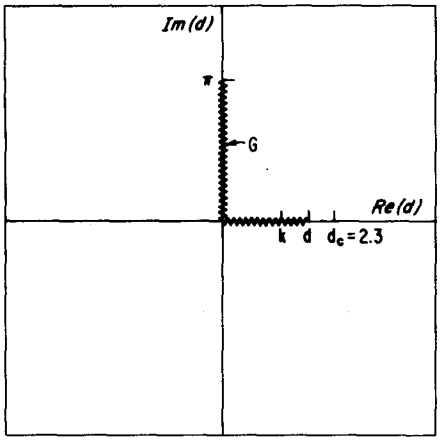

FIG. 6. In the complex d plane (d is the cumulative wavenumber), the wiggly line G presents the path of $d(Y)$ that produces the same complex phase speed for all meridional sections.

Substituting $l(Y)$ from (3.3) into (3.4) and taking $c = ic_i$ as we are investigating instabilities (i.e., $k < d_c$), we get after integration:

$$2L[(\pi^2+k^2)(A^2+B^2)]^{1/2}\left[K\left(\frac{A}{A^2+B^2}\right) - E\left(\frac{A}{A^2+B^2}\right)\right] = \pi\left[n+\frac{1}{2}\right] \quad (3.5)$$

where

$$A^2 = \frac{d_c^2-k^2}{4c_i^2(\pi^2+k^2)q} - \frac{1}{q}$$

$$B^2 = \frac{1}{4c_i^2 q}$$

K complete elliptic integral of the first kind
E complete elliptic integral of the second kind

$$x = \frac{A}{(A^2+B^2)^{1/2}}$$

When $x < 1$, we can approximate

$$E(x) \approx \frac{\pi}{2}\left(1+\frac{x^2}{4}\right)$$

$$K(x) \approx \frac{\pi}{2}\left(1+\frac{x^2}{4}\right).$$

Far from the neutral point, x is rather small and after a bit of algebra we derive that the growth rate is approximately

$$c_i^2 = \frac{d_c^2-k^2}{(4(\pi^2+k^2))}\left[1-\frac{(2n+1)q^{1/2}}{L(d_c^2-k^2)^{1/2}}\right], \quad (3.6)$$

which can be written as

$$c_i^2 = [c_{iE}(\text{at the center})]^2\left[1-\frac{(2n+1)q^{1/2}}{L(d_c^2-k^2)^{1/2}}\right]. \quad (3.7)$$

The c_{iE} (at the center) denotes the eigenvalue of the local problem at the center of the jet for $l = 0$. Eigenrelation (3.7) thus relates the homogeneous Eady problem to the nonhomogeneous one. In the limit $L \to \infty$ we capture the dispersion of the homogeneous Eady problem. Figure 7 shows the growth rate for the homogeneous Eady problem, while Figs. 8a, b the growth rates for a variety of Ros. The symmetric and antisymmetric modes are such that the growth rate of a lower mode is always larger than for higher modes.

Expression (3.7) can also be written in the form of the dispersion relation for the homogeneous problem, with the wavenumber now being $k^2 + \bar{l}^2$, $\bar{l}^2$ is the mean meridional wavenumber, and considering $\bar{l}^2$ a small quantity we get

$$\bar{l} = \frac{(2n+1)^{1/2}}{L^{1/2}}\left[\frac{[(d_c^2-k^2)q]^{1/2}}{(\pi^2+d_c^2)(\pi^2+k^2)}\right]^{1/2}. \quad (3.8)$$

Hence the disturbance influences a distance $(L)^{1/2}$, or, dimensionally $(La)^{1/2}$, which is the geometric ratio of the scale of variation of the jet and the Rossby radius of deformation; a result in accord with Gent (1974, 1975) and Simmons (1974).

The reduction of maximum growth rates associated with higher Ros, as seen in Figs. 8a, b, is related to the larger $\bar{l}$ that occurs when Ros is increasing. The variation of the maximum growth rate with Ros is depicted in Fig. 9, where the first symmetric and antisymmetric modes are shown.

For a specific L, the modes that are strongly unstable must be such that $L > (2n + 1)$, where n is the mode index. When the previous inequality is violated our theory does not suffice; higher order perturbation theory is needed. However, McIntyre (1970), using higher order theory, showed that these high wavenumber modes are only weakly unstable.

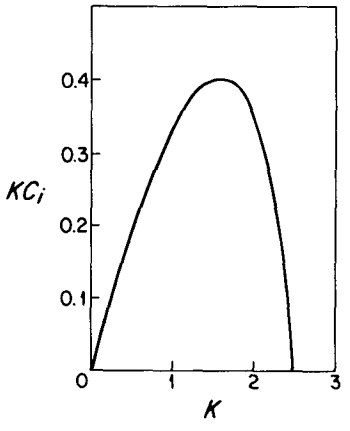

FIG. 7. The growth rate, kc_i for the homogeneous Eady problem as a function of zonal wavenumber k. The variables are nondimensional.

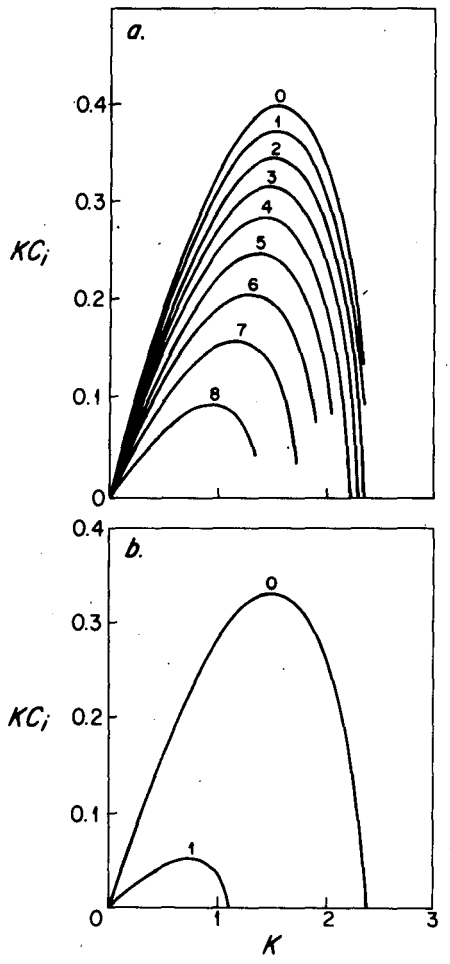

FIG. 8. The growth rate, kc_i for the nonhomogeneous Eady problem as a function of zonal wavenumber. The variables are nondimensional. The zonal wind is taken to be of the form: $l/(l + Y^2)$. (a) is for a jet with Ros = 0.1 and, (b) for a jet with Ros = 0.6. The labels on the curves signify the order of the meridional mode. 0 is the first symmetric, 1 for the first antisymmetric, 2 for the second symmetric mode, etc.

4. The Charney problem

The Charney problem consists of finding the solution of Eq. (A) and (B) in their full form, with the upper boundary condition located at infinity. The only difference with the problem solved by Charney (1947) is that the cumulative wavenumber $k^2 + l^2(Y, c)$ is complex. The solution of (A) that yields the dispersion relation $D(c, k, l(Y, c))$, which can be written in terms of Whittaker functions or established numerically. The calculation with Whittaker functions has been performed, but the computation burden is large; we must bear in mind that the vertical Eq. (A) has to be solved at all the meridional mesh points to provide adequate numerical description of $l^2(Y, c)$, to enable the integration of (B) so as to determine the new estimate of c in the Newton process.

Fortunately Lindzen and Rosenthal (1981), hereafter referred to as LR, give an highly accurate W.K.B.J. solution for the baroclinic problem, which is valid in the complex plane.

Their dispersion relation takes the form:

$$\left[\frac{1}{2}+\frac{1}{c'}-\left(\frac{[d^2+(r'+1)/c']^{1/2}}{x(c')}+\frac{r'+1}{4c'^2[d^2+(r'+1)/c']}\right)\right]$$
$$=\left\{-2\frac{\sin(\pi-Z_t)}{\exp[i(\pi-Z_t)]}K_l'[x(c')]+I_l'[x(c')]\right\}$$
$$-[d^2+(r'+1)/c']^{1/2}\left[-2\frac{\sin(\pi-Z_t)}{\exp[i(\pi-Z_t)]}K_l'[x(c')]\right.$$
$$\left.+I_l'[x(c')]=0\right.$$

where

$$d^2=k^2+l^2(Y,c)+\tfrac{1}{4}$$

$$Z_t=\frac{r+\bar{u}(Y)}{2d}$$

$$r'=\frac{r}{\bar{u}(Y)}$$

$$c'=\frac{c}{\bar{u}(Y)}$$

$$x(c')=c'[d^2+(r'+1)/c']^{1/2}$$
$$+\frac{r'+1}{d}\ln\{[c'/(r'+1)]^{1/2}[d^2+[d^2+(r'+1)/c']^{1/2}]\}$$

Here K_l, I_l, K_l', I_l' are Bessel functions of imaginary order and their corresponding derivatives.

The results that will be discussed will pertain to a jet of the form:

$$\bar{u}(y)=(1-\text{Ped})\exp(-Y^2)+\text{Ped}.$$

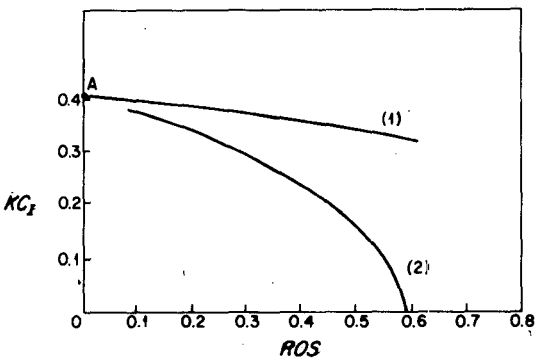

FIG. 9. The growth rate, kc_i, as a function of Ros. This graph shows the uniform approach of the growth rate of the Eady problem with a jet, to that with no latitudinal variation. The growth rate in the absence of latitudinal variation corresponds to point A. The zonal wavenumber is k = 1.6. Curve (1) plots the variation for the first symmetric mode while curve (2) is for the first antisymmetric mode.

Numerous comparative calculations have been made which show that the accuracy of c obtained using the LR dispersion relations is actually greater for the inhomogeneous case than for the homogeneous case. Moreover, the use of truncated Bessel function approximations is more accurate than the use of "exact" Whittaker function expressions at the same level of truncation.

Even when the dispersion relation has been severely truncated to two terms in the Bessel function expansions, good agreement with the results obtained with the "exact" dispersion was achieved. This result is demonstrated by comparing Fig. 10b with Fig. 14a, both pertaining to the first symmetric mode. This realization can be the vehicle for performing intricate instability calculations of continuous atmospheric flows with a minimum of computer time.

It should be noted that although the LR expressions are excellent in approximating the eigenvalues, they are not to be used in a numerical integration of the vertical equation. If a LR eigenvalue is substituted in (A) and subsequently (A) is numerically integrated in the vertical, the solution will exponentially increase with height. Hence, to determine the vertical structure of a disturbance we must adhere to the W.K.B.J. eigenfunctions derived in LR. The W.K.B.J. expressions involve the matching of Bessel functions with Airy functions, and they are not easy to use. Instead we have employed Whittaker functions for the determination of the vertical structures and their associated second-order quantities (the eddy-fluxes: momentum, heat and potential vorticity).

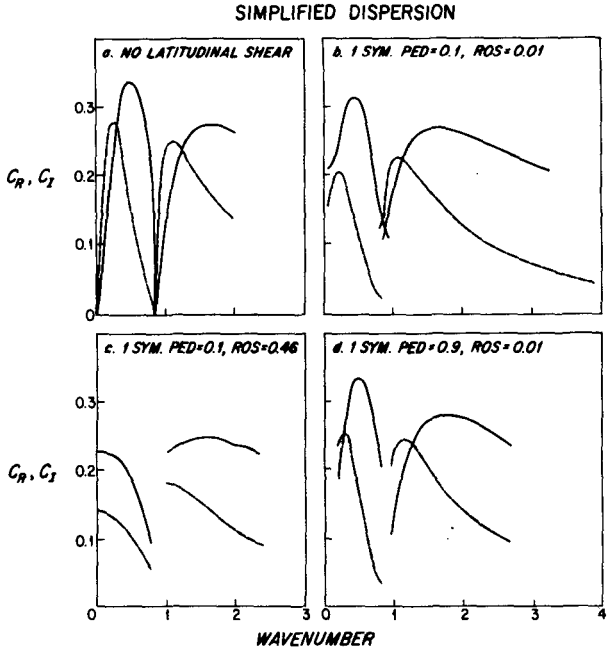

FIG. 10. Plot of phase speed as a function of k. The continuous curve is the real part, c_r, and the imaginary part, c_i, is the discontinuous curve. The variables are nondimensional. This is the solution of the Charney problem with the presence of various jets. The Charney dispersion relation has been here simplified by a two term expansion of the Bessel functions in the approximate dispersion relation of Lindzen and Rosenthal. (a) is for a zonal flow with no latitudinal variation, (b) the zonal wind is a jet with Ros = 0.01 and Ped = 0.1, (c) Ros = 0.46 and Ped = 0.1, (d) Ros = 0.01 and Ped = 0.9.

a. Growth rates and phase speeds of unstable modes

We will present growth rates and phase speeds for a variety of values of Ros and pedestal values for the first three meridional modes: the first and second symmetric and the first antisymmetric. There are two ways of approaching a uniform flow; we will refer to these as the geometric and the dynamic. In the geometric approach, the pedestal value is increased so that the jet finally disappears and becomes a uniform velocity profile. In the dynamic approach the region of influence of the motions in the meridional direction, as given in quasi-geostrophic theory by Ros, reduces to make the disturbance exist in what is essentially a uniform flow. Both limit cases are shown in Figs. 11a, b and the approach to the case of uniform flow is demonstrated; in both cases the growth rate is increasing with the decrease of the effective barotropicity.

As we have remarked in the Introduction, the presence of the jet will self-consistently determine a meridional wavenumber l for a disturbance of given longitudinal wavenumber k. This l depends on k and varies slowly with latitude (refer to Fig. 16). The real value of l at the center of the jet $l(0)$ turns out to be of particular importance. If we take the dispersion curves of Charney and plot them against $[k^2 + l^2(0)]^{1/2}$, as was done in the introduction, where $l(0)$ is the appropriate wavenumber for a given jet, we find remarkable agreement with the dispersion curves that result from the complete numerical solution (refer to Figs. 2, 12, 13 and 14).

The dependence of $l(0)$ on k is weak and progressively weakens as we consider higher meridional modes (Fig. 15a, b, c). From Fig. 15, it is evident that for small enough k there is the possibility for the selection of a small enough $l(0)$ that can result in a $[k^2 + l^2(0)]^{1/2} < 0.75$ and permit the existence of instability modes that exhibit vertical structures akin to the Burger modes. For these modes the dependence of $l(0)$ on k is rather dramatic, given they must satisfy the above inequality. The Burger modes have a meridional variation that is slower, producing disturbances that are wider in the latitudinal extent. These disturbances should be compared to the ones with larger l that exhibit vertical structures like those of the Charney modes and satisfy $[k^2 + l^2(0)]^{1/2} > 0.75$. The Charney modes decay rapidly in the meridional direction (viz., Fig. 16).

There is the distinct possibility of having a multivalued dispersion relation for a given meridional mode. These modes are either contiguous to the Charney

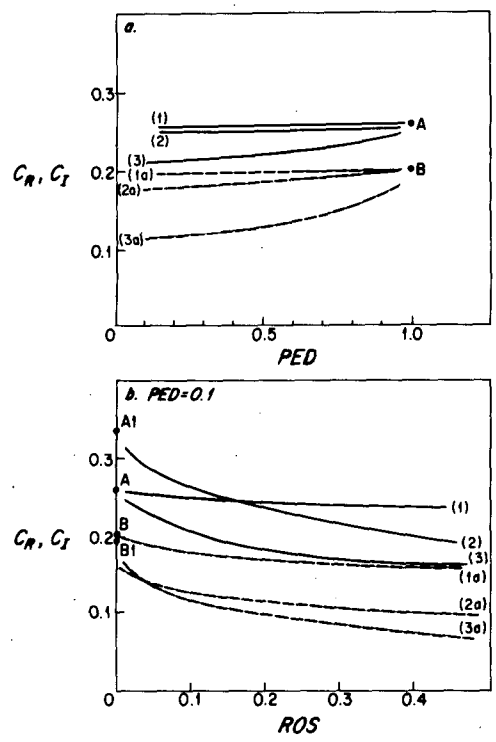

FIG. 11. (a) Plot of c_r (continuous curves 1, 2, 3) and c_i (discontinuous curves 1a, 2a, 3a) with respect to Ped for $k = 1.5$. Curves 1, 1a refer to the first symmetric mode for Ros = 0.01. Curves 2, 2a refer to the first symmetric mode for Ros = 0.01. Curves 3, 3a refer to the second symmetric mode for Ros = 0.1. Point A represents the value of c_r and point B the c_i for the homogeneous Charney problem. (b) Plot of c_r (curves 1, 2, 3) and c_i (curves 1a, 2a, 3a) with respect to Ros for Ped = 0.1. Curves 1, 1a refer to the first symmetric mode for $k = 1.5$. A, B represent the corresponding values of c_r and c_i of the homogeneous Charney problem for $k = 1.5$. Curves 2, 2a refer to the first symmetric mode for $k = 0.5$. A1, B1 represent the corresponding values of c_r and c_i of the homogeneous Charney problem for $k = 0.5$. Curves 3, 3a refer to the second symmetric mode for $k = 1.5$.

mode or the Burger mode, and their corresponding $l(0)$ are such as to satisfy the inequality characteristics for each case. Such a multivalued dispersion relation for the first antisymmetric meridional mode is demonstrated in Fig. 13. It is worth noting that the presence of meridional shear in the jet prohibits the existence of any waves with $c_r = c_i = 0$. For a proof, refer to Appendix 1.

The fastest growing modes are the ones that are contiguous to the Charney mode. For these we empirically have (refer to Fig. 18)

$$l(0) = 1.8(2n+1)^{1/2}(\mathrm{Ros})^{0.4},$$

where n is the meridional mode index ($n = 0$ for the first symmetric mode). To obtain the above expression we have averaged over the k variation, which in this domain of instability is a weak one. This further means that the turning points of Eq. (B), namely the region of confinement, are weakly dependent on the wavenumber k and the meridional mode.

It was mentioned earlier that severe truncations of the LR approximations yield results very close to the calculations employing the full LR dispersion relation. Figures 10 attest to that, but further show the transition from the spectrum of a uniform flow to various nonuniform configurations; in these very rapid calculations the two-term expansion of LR has been used. These two-term calculations are an order of magnitude faster than the calculations that employ Bessel function approximations to the Whittaker functions and are, in turn, an order of magnitude faster than the calculations that employ the Whittaker functions.

In Figs. 17a, b the growth rates and frequencies of the first three meridional modes are plotted for a variety of jet configurations. Note that the maximum growth rate is achieved at about $k = 1.5$ (dimensional wavelength 4000 km) and approximately in the region $0.4 < k < 0.9$ (dimensional wavelength between 16 000 km and 7000 km). The highest growing mode is the first antisymmetric (except in Fig. 17a, the case of a very broad jet, where the fastest growing mode becomes the second symmetric). In the neighborhood of $k = 0$ the fastest growing mode is again the first symmetric.

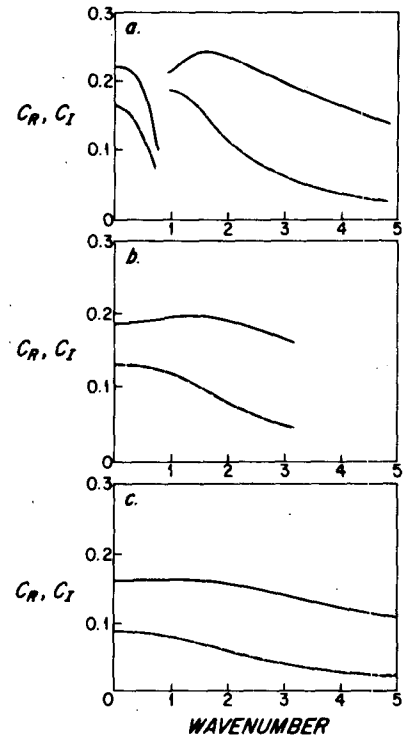

FIG. 12. Plot of c_r (continuous curve) and c_i (discontinuous curve) as a function of k, for the Charney problem in a zonal flow with Ros = 0.5 and Ped = 0.1. (a) is the first symmetric mode, (b) the first antisymmetric mode and (c) the second symmetric mode. For this calculation the full LR dispersion relation has been employed.

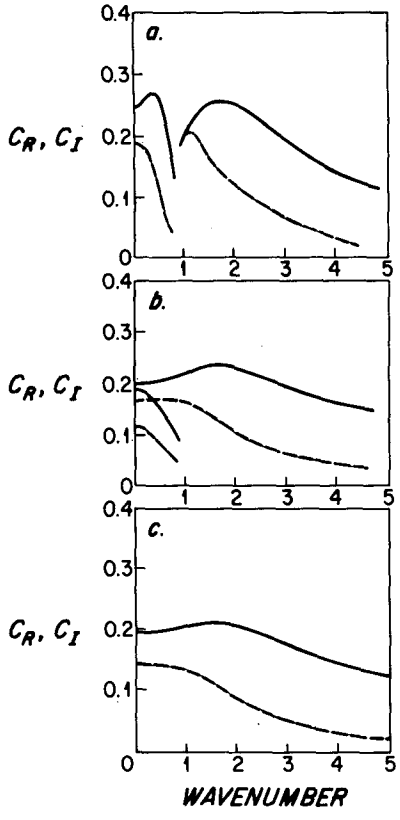

FIG. 13. As in Fig. 12 but now the zonal flow has Ros = 0.1 and Ped = 0.1.

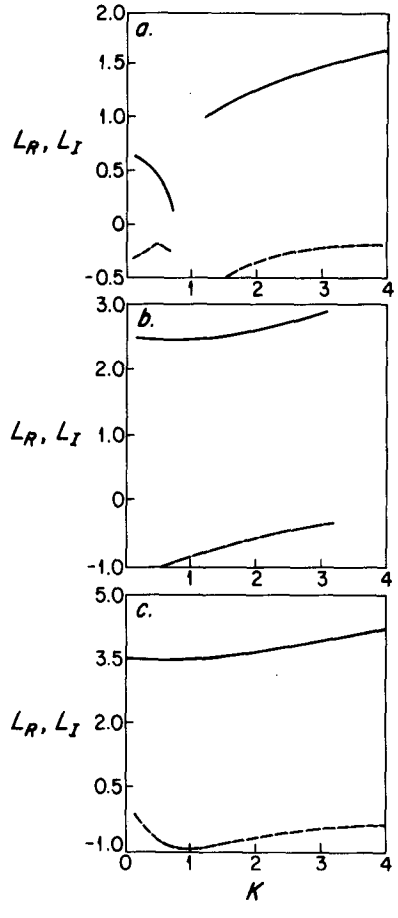

FIG. 15. Plot of the meridional wavenumber as a function of zonal wavenumber. The continuous curve is the real part LR and the discontinuous curve is the imaginary part. The jet has Ros = 0.5 and Ped = 0.1. (a) is for the first symmetric mode; (b) the first antisymmetric, and (c) is the second symmetric mode.

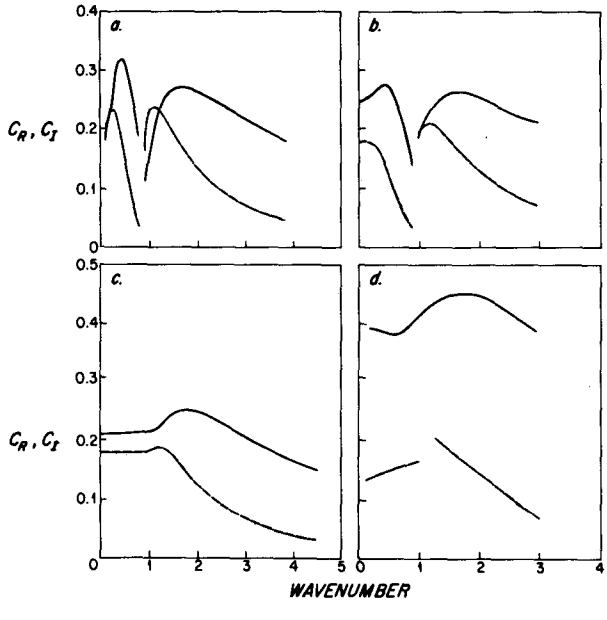

FIG. 14. As in Fig. 12 but now the zonal flow has Ros = 0.01 and Ped = 0.1. Plot (d) is the spectra of the fastest growing modes of the 30° jet of Simmons and Hoskins (1976).

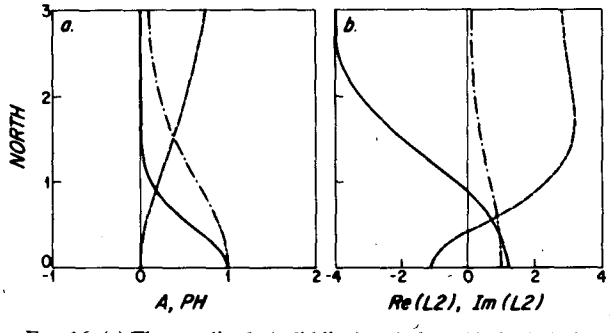

FIG. 16. (a) The amplitude (solid line) and phase (dash–dash line) of the first symmetric unstable mode with $k = 3$ is plotted against meridional distance to the north of the center of the jet. The jet (Ros = 0.5, Ped = 0.1) is also plotted in the background (dash–dot line). The scale of the latitude north is measured in the units of Y [related to dimensional y by $y = (a/\text{Ros})Y$]. For the phase, 1 corresponds to 180. The disturbance is normalized to be of amplitude 1 and phase 0 at its maximum. (b) For the same disturbance the variation of the meridional wavenumber, real (solid line) and imaginary (dash–dash line) parts, with latitude as in (a).

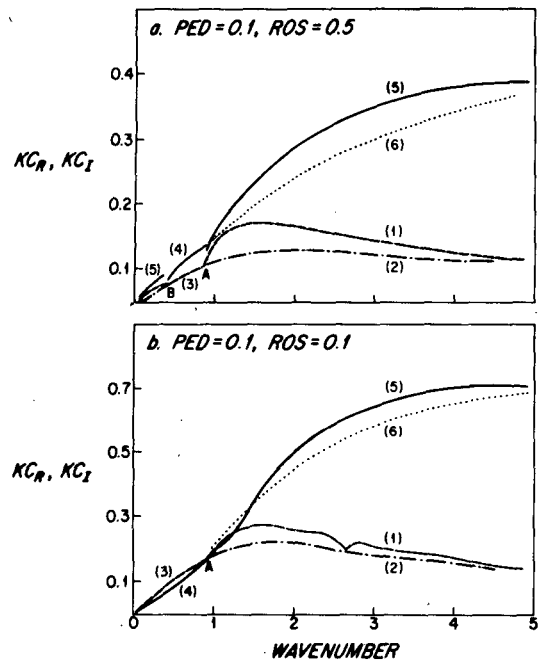

FIG. 17. Plot of the real frequency (kc_r) and growth rate (kc_i) as a function of zonal wavenumber k. Curve 5 is a graph of kc for the first symmetric mode, while 6 and 4 are for the first antisymmetric mode. Curve 1 is a graph of growth rate for the first symmetric mode, while 2 and 3 are for the first antisymmetric mode. The continuous curve shows the real frequency (kc_r) and corresponds to the fastest growing mode for each k. At the wavenumber corresponding to point A, the fastest growing mode becomes the first antisymmetric mode and at point B the first symmetric mode is again growing fastest. Plot (a) corresponds to a jet with Ros = 0.5 and Ped = 0.1 while (b) corresponds to Ros = 0.1 and Ped = 0.1.

This discontinuity of the spectra has also been found by Simmons and Hoskins (1976), where it was also noted that at these wavelengths a higher meridional mode is most unstable. Figures 12a, b, c provide the spectra of an instability of a jet that realistically corresponds to an atmospheric flow. These spectra can be compared to the ones that Simmons and Hoskins (1976) derived for the 30° jet, after integrating the quasi-geostrophic equations on a sphere. The result of their integration is presented for comparison in Fig. 14d. The imaginary part of the phase speed is very close to ours, but there is an appreciable discrepancy in the real part of the phase speed. This may be due to the fact that they are using a layer model.

b. Remarks on Killworth (1980)

In the above calculations for the Eady and Charney problems, it was noted that as the limit of homogeneous flow was taken, the results asymptotically approached those of the homogeneous problem. Moreover, for finite jets the results were interpretable in terms of the results of the homogeneous problem, provided a meridional wavenumber was included—the meridional wavenumber being determined by the jet.

In all cases, the results of the homogeneous calculations remain clearly relevant. We mention this only because the work of Killworth (1980) suggests that the approach of jet cases to the homogeneous results is "nonuniform," the further implication being that the results of the homogeneous calculations might prove irrelevant when meridional shear is present.

By "uniform approach" Killworth (1980) meant that a real latitude, Y_0, existed at which the local (homogeneous) instability properties coincided with those of the jet. In the case of a symmetric jet, this was clearly the case for the Eady problem. On the other hand, for the Eady problem with an asymmetric jet or for the Charney problem with any jet, the appropriate Y_0 is, in fact, complex. Killworth (1980) referred to such cases as "nonuniform." Nevertheless, even in these cases we have seen that the homogeneous results were asymptotically approached in the limit of homogeneous flow. More important, even in the presence of a finite jet, the connection of the jet results to those of the homogeneous problem were always clear.

5. Modification of the flow

Unstable waves transport heat, momentum and potential vorticity. These fluxes can be readily calculated from the unstable normal modes (refer to Pedlosky, 1979). In Fig. 19 we show a typical meridional section of the structure of the unstable wave k = 1.6, Ros = 0.1 and the associated heat, potential vorticity and momentum fluxes.

Heat fluxes are northward with a maximum at the ground. Slight southward heat fluxes are observed and

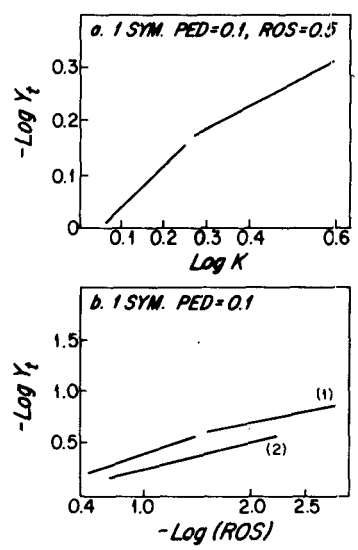

FIG. 18. (a) Graph of $-\log(Y_i)$ as a function of $\log(k)$, $k > 1$. Y_i is the half-width of the eigensolution. The graph is for the first symmetric mode in a jet of Ros = 0.5, Ped = 0.1. (b) Graph of $-\log(Y_i)$ as a function of $-\log(\text{Ros})$. Curve 1 corresponds to k = 2.2 while curve 2 to k = 1.5, both for the first symmetric mode.

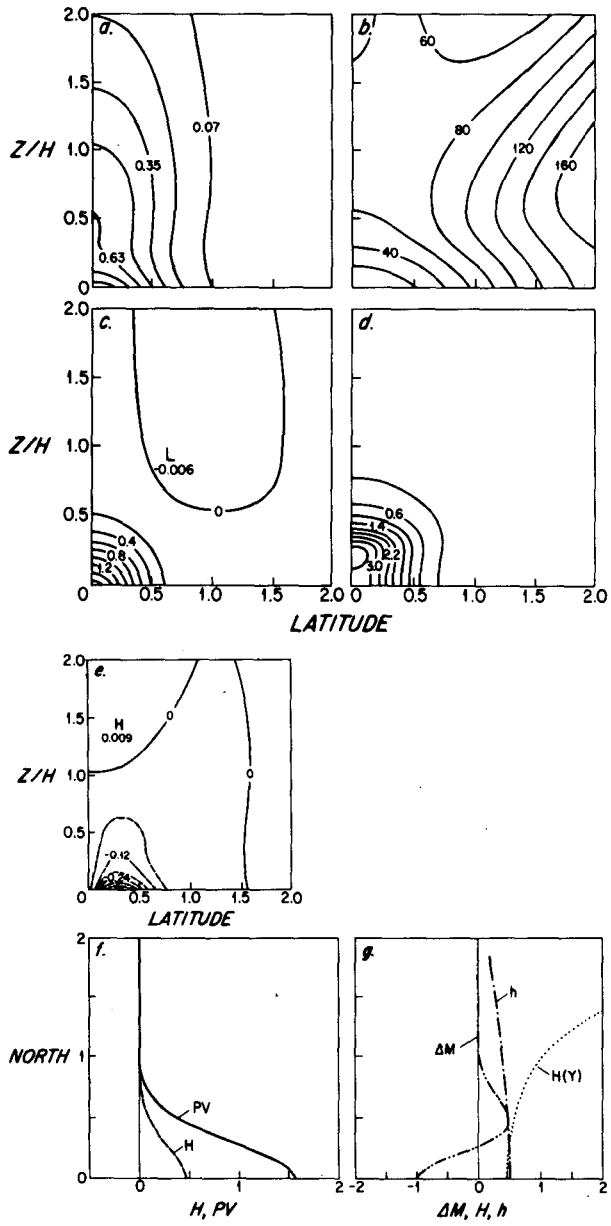

FIG. 19. Contour plots (a) of the amplitude, (b) of the phase, (c) heat flux, (d) potential vorticity flux, (e) momentum flux as a function of height and latitude. Height is measured in scale heights, H. The disturbances have been normalized to have amplitude 1 and phase 0 at the center of the jet. The latitude is measured north of the center of the jet. It is measured in units of the slow variable Y. All quantities are nondimensional. Graph (f) presents the variation of the height integrated heat (H) and potential vorticity (PV) flux as a function of latitude Y north of the center of the jet. Graph (g) is the vertically integrated momentum flux convergence (ΔM) as a function of Y, normalized to be 1 at the center of the jet. The plots are for the first symmetric mode with $k = 1.6$ in a jet with Ros = 0.5, Ped = 0.1. Other curves are defined in Appendix B.

they are due to the eastward tilt of the phase of the perturbation at the wings of the jet (see also Simmons and Hoskins, 1976).

Potential vorticity fluxes have their maximum at a height z = Real (c).

The detailed structure of the momentum fluxes can be complicated. Invariably there is maximal convergence at the maximum of the perturbation streamfunction, but there may be weak divergence higher. While the detailed structure of the momentum fluxes is complicated, the vertically integrated eddy momentum flux convergence (M_y) turns out to be simple to describe. Furthermore, this quantity primarily controls the back effect of the unstable wave on the zonal flow.

It can be proved that (refer to Appendix 2)

$$M_y = \frac{k\,\mathrm{Im}(l^2)}{4}\int_0^\infty |\psi|^2 dz. \tag{5.1}$$

The above expression leads to the interpretation of the solvability condition (2.14) as that of conservation of momentum. Further, it can be proved (refer to Pedlosky, 1975) that the vertically averaged acceleration of the mean zonal field A is

$$A = -M_y. \tag{5.2}$$

In other words the acceleration from the meridional circulation, induced by the heat fluxes, averages to zero in the vertical.

For the first symmetric mode, the typical distribution of A is shown in Fig. 19g. Such a distribution implies that a column of fluid situated at the center of the jet will be accelerated, while a column at the wings of the jet will be decelerated. The jet maximum will get enhanced and the barotropicity of the flow, as measured by the latitudinal shear, will increase. The interaction is weaker for broader jets and asymptotically as the jet has no meridional shear; the mean acceleration tends to zero in accord with the noninteraction theorem. For example, similarly normalized unstable waves ($k = 1.6$) will have, at the center of the jet accelerations, the ratio of 0.22:0.14:0.04 respectively for Ros = 0.5, 0.1, 0.01.

The typical effect of the first antisymmetric mode is shown in Fig. 21. Here again the barotropicity increases while the curvature at the center of the jet increases.

To complete the picture of the modification of the zonal flow, the effect on the shear at the bottom must be calculated. The bottom shear regulates baroclinic instability (refer to Lindzen et al., 1980).

The acceleration of the shear A_z at the ground is given by the latitudinal curvature of northward eddy heat flux H:

$$A_z = H_{yy}|_{z=0}. \tag{5.3}$$

A version of the above relationship in spherical coordinates appears in Simmons and Hoskins (1976). In Fig. 20 we show the typical acceleration of the shear of the mean zonal flow induced by the first mode. At the center of the jet the ground shear is reduced, the baroclinicity is reduced, and at the wings of the jet the shear is enhanced.

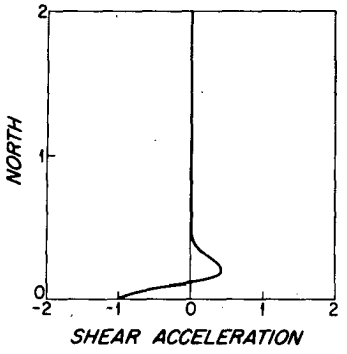

FIG. 20. Graph of the acceleration of the wind shear at the ground as a function of latitude north of the center of the jet using the first symmetric mode with $k = 3$, Ros = 0.01 and Ped = 0.1.

On the assumption that the instability manifests itself primarily in the gravest mode, the modified flow will possess smaller baroclinicity at the center of the jet and higher Ros. This leads to a reduction of the growth rate.

6. Conclusions

This paper was principally concerned with the inclusion of a meridional jet in the Charney model of instability.

We have presented a numerical scheme that efficiently determines the spectra, structure and fluxes associated with the unstable disturbances. The method unveils the instability characteristics of the various meridional modes, extending the stability analyses of complicated realistic flows that determine only the fastest growing mode.

We found that jets act to confine the instability meridionally and, once the internally determined meridional wavenumber is taken into account, the spectra approximately correspond to the classical results without a jet. We should note that the disturbances are more confined at lower levels. It is also demonstrated that the instability of a jet uniformly approaches the instability of a flow with no meridional variation.

However, unlike the classical results the neutral waves are suppressed and the Burger and Charney modes can coexist. The Burger modes are also suppressed for tight jets. The meridional wavenumber is complex and we have proved that the imaginary part is responsible for the back effect on the mean flow. The effect on the mean flow is to reduce the baroclinicity at the ground while the jet is barotropically concentrated, potentially paving the way for the manifestation of barotropic instability. Our analysis would then be invalid as we have filtered out barotropic instabilities.

The maximal growth occurs around global zonal wavenumber 8; this feature is weakly dependent on the jet width. Maximally growing waves are in the first meridional mode. The presence of the jet reduces the growth rate of the instability. Higher meridional modes grow in general slower, given that the corresponding meridional wavenumber is larger. The situation is different for small zonal wavenumbers where the fastest growing waves are in the first antisymmetric meridional mode. It is these waves that now have the meridional extent of the jet.

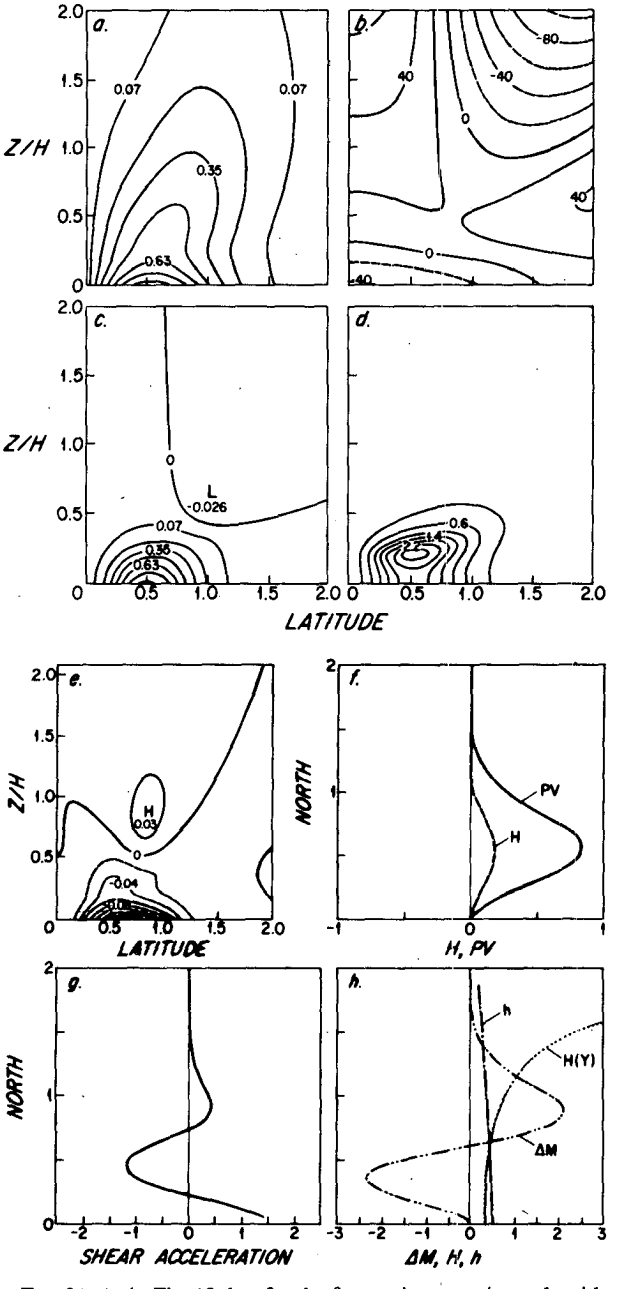

FIG. 21. As in Fig. 19, but for the first antisymmetric mode with $k = 1.6$, Ros = 0.5. (a) is the amplitude, (b) the phase, (c) the heat flux, (d) the potential vorticity flux and (e) the momentum flux. Graph (f) is the variation of height integrated heat (H) and potential vorticity flux (PV) as a function of latitude. Graph (g) is the variation of the acceleration of the wind shear at the ground with latitude and (h) the vertically integrated momentum flux convergence (ΔM) as a function of latitude; other curves are defined in Appendix B.

It should be noted that the approximate dispersion relation derived by Lindzen and Rosenthal (1981) performs accurately. This dispersion relation can be the vehicle for performing similar calculations for zonal flows with more realistic height dependence. Similarly, the same methodology can be used for the investigation of the instability of asymmetric zonal flows.

Finally we address the question of whether these normal modes are realizable. We can heuristically assume that a random perturbation will not mature into a normal mode when its local growth rate is far bigger than the time it needs to travel a distance of the order of the meridional inhomogeneity. Such a consideration determines that our analysis is valid for waves with global zonal wavenumbers smaller than 12–13. Shorter waves seem to grow as if they were in a uniform medium. Hence, it seems that the propagation of baroclinic wave pulses is affected by the jet structure only when the long wave components are involved (Farrell, 1982).

Acknowledgments. This work was supported by NSF Grant 8342482 and NASA Grant NAGW-525, as well as the predecessors of these grants. The work is based on the Ph.D. thesis of Petros Ioannou at Harvard University.

APPENDIX A

The Impossibility of Neutral Waves in a Jet

As has been pointed out in Lindzen et al. and in LR, neutral modes ($c = 0$) for the Charney problem exist if and only if $d = (k^2 + l^2(Y) + 1/4)^{1/2}$ satisfies the relation:

$$\pi\left[\frac{r(\bar{u}(Y)+1)}{d}\right]=2n\pi, \quad n=0,\pm1,\pm2,\cdots. \tag{A1}$$

The existence of such a mode depends on whether there exists a $l(Y)$ consistent with (A1) that simultaneously satisfies Eq. (B). Solving (A1) for $l^2(Y)$ we get

$$l^2(Y)=\frac{[r/u(Y)+1]^2}{4n^2}-k^2-\frac{1}{4}. \tag{A2}$$

Equation (B) becomes

$$\frac{d^2W}{dY^2}+L^2\left[\frac{[r/\bar{u}(Y)+1]^2}{4n^2}-k^2-\frac{1}{4}\right]W=0 \tag{A3}$$

for $n = 0, \pm1, \pm2, \cdots, W \to 0$ as $|Y| \to \infty$.

Such a solution exists if $l^2(Y)$ changes sign and is negative at infinity. But if $\bar{u}(Y)$ is jetlike (i.e., $u(\bar{Y})$), monotonically decreasing, $l^2(Y)$ will be monotonically increasing, and thus cannot satisfy the requirements for a solution. We observe that neutral solutions can exist if $\bar{u}(Y)$ is increasing, so that an appropriate trapped region appears in (A2). As a result, the dispersion cannot provide for c_r and c_i simultaneously vanishing.

APPENDIX B

Momentum Relation

Held (1978) proves:

$$My=-[\rho_0\overline{vq}]_{z=0}[H(Y)-h(Y)] \tag{B1}$$

where M_y is the height integrated momentum flux convergence.

The $\overline{vq}$ northward potential vorticity flux

$$H(Y)=\frac{\int_0^\infty \rho_0\overline{vq}dz}{[\rho_0\overline{vq}]_{z=0}}$$

is average over a period

$$h(Y)=\frac{1}{1+r'} \quad \text{and} \quad r'=\frac{r}{\bar{u}(Y)}.$$

Substituting into (B1) and using (A) of section 2, we can prove:

$$H(Y)-h(Y)=\frac{\mathrm{Im}(l^2)}{r'+1}\frac{|c'|^2}{c_i'}\frac{\int_0^\infty(\psi)^2dz}{[|\psi|^2]_{z=0}}$$

where $c' = c/u(Y)$, hence

$$M_Y=\frac{k\,\mathrm{Im}(l^2)}{4}\int_0^\infty|\psi|^2dz.$$

REFERENCES

Bender, C. M., and S. A. Orszag, 1978: *Advanced Mathematical Methods for Scientists and Engineers.* McGraw-Hill, 593 pp.

Burger, A. P., 1962: On the non-existence of critical wavelengths in a continuous baroclinic stability problem. *J. Atmos. Sci.*, **19**, 31–38.

Charney, J. G., 1947: The dynamics of long waves in a baroclinic westerly current. *J. Meteor.*, **4**, 135–162.

——, and M. E. Stern, 1962: On the stability of internal baroclinic jets in a rotating atmosphere. *J. Atmos. Sci.*, **19**, 159–172.

Eady, E. J., 1949: Long waves and cyclone waves. *Tellus*, **1**, 33–52.

Erderlyi, A., 1956: *Asymptotic Expansions.* Dover, 108 pp.

Farrell, B. F., 1982: Pulse asymptotics of the Charney baroclinic instability problem. *J. Atmos. Sci.*, **39**, 507–517.

Frederiksen, J. S., 1978: Instability of planetary waves and zonal flows in two layer models on a sphere. *Quart. J. Roy. Meteor. Soc.*, **104**, 841–872.

Gent, P. R., 1974: Baroclinic instability of a slowly varying flow. *J. Atmos. Sci.*, **31**, 1983–1994.

——, 1975: Baroclinic instability of a slowly varying flow, Part 2. *J. Atmos. Sci.*, **32**, 2094–2102.

Green, J. S. A., 1960: A problem of baroclinic stability. *Quart. J. Roy. Meteor. Soc.*, **86**, 237–251.

Held, I. M., 1978: The vertical scale of an unstable baroclinic wave and its importance for eddy heat flux parameterizations. *J. Atmos. Sci.*, **35**, 572–576.

Hoskins, B. J., and M. J. Revell, 1981: The most unstable long wavelength baroclinic instability modes. *J. Atmos. Sci.*, **38**, 1498–1503.

Killworth, P. D., 1980: Barotropic and baroclinic instability in rotating, stratified fluids. *Dyn. Atmos. Oceans*, **4**, 143–184.

——, 1981: Eddy fluxes and mean flow tendencies in open-ocean baroclinic instability. *Dyn. Atmos. Oceans*, **5**, 175–186.

Kuo, H. L., 1979: Baroclinic instabilities of linear and jet profiles in the atmosphere. *J. Atmos. Sci.*, **36**, 2360–2378.

Lindzen, R. S., and K.-K. Tung, 1978: Wave overreflection and shear instability. *J. Atmos. Sci.*, **35**, 1626–1632.

——, and ——, 1980: A simple approximate result for the maximum growth rate of baroclinic instability. *J. Atmos. Sci.*, **37**, 1648–1654.

——, and H. L. Kuo, 1969: *Mon. Weather Rev.*, **97**, 732–734.

——, and A. J. Rosenthal, 1981: A WKB asymptotic analysis of baroclinic instability. *J. Atmos. Sci.*, **38**, 619–629.

——, B. Farrell and K.-K. Tung, 1980: The concept of wave overreflection and its application to baroclinic instability. *J. Atmos. Sci.*, **37**, 44–63.

Lorenz, E. N., 1967: *On the Nature and Theory of The General Circulation of the Atmosphere.* World Meteorological Organization (United Nations) Geneva, Publ. No. 218, T.P. 115, 161 pp.

McIntyre, M. E., 1970: On the non-separable baroclinic parallel flow instability problem. *J. Fluid Mech.*, **40**, 273–306.

Miles, J. W., 1964: Baroclinic instability of the zonal wind. *Rev. Geophys.*, **2**, 155–176.

Niehaus, M. C. W., 1980: Instability of nonzonal baroclinic flows. *J. Atmos. Sci.*, **37**, 1447–1463.

——, 1981: Instability of nonzonal baroclinic flows: Multiple-scale analysis. *J. Atmos. Sci.*, **38**, 974–987.

Pedlosky, J., 1979: *Geophysical Fluid Dynamics*, Springer-Verlag, 624 pp.

——, 1975: On secondary baroclinic instability and the meridional scale of motion in the sea. *J. Phys. Oceanogr.*, **5**, 603–614.

Simmons, A. J., 1974: The meridional scale of baroclinic waves. *J. Atmos. Sci.*, **31**, 1515–1525.

——, and B. J. Hoskins, 1976: Baroclinic instability on the sphere: Normal modes of the primitive and quasi-geostrophic equations. *J. Atmos. Sci.*, **33**, 1454–1477.

Stone, P. H., 1969: The meridional scale of baroclinic waves. *J. Atmos. Sci.*, **26**, 376–389.